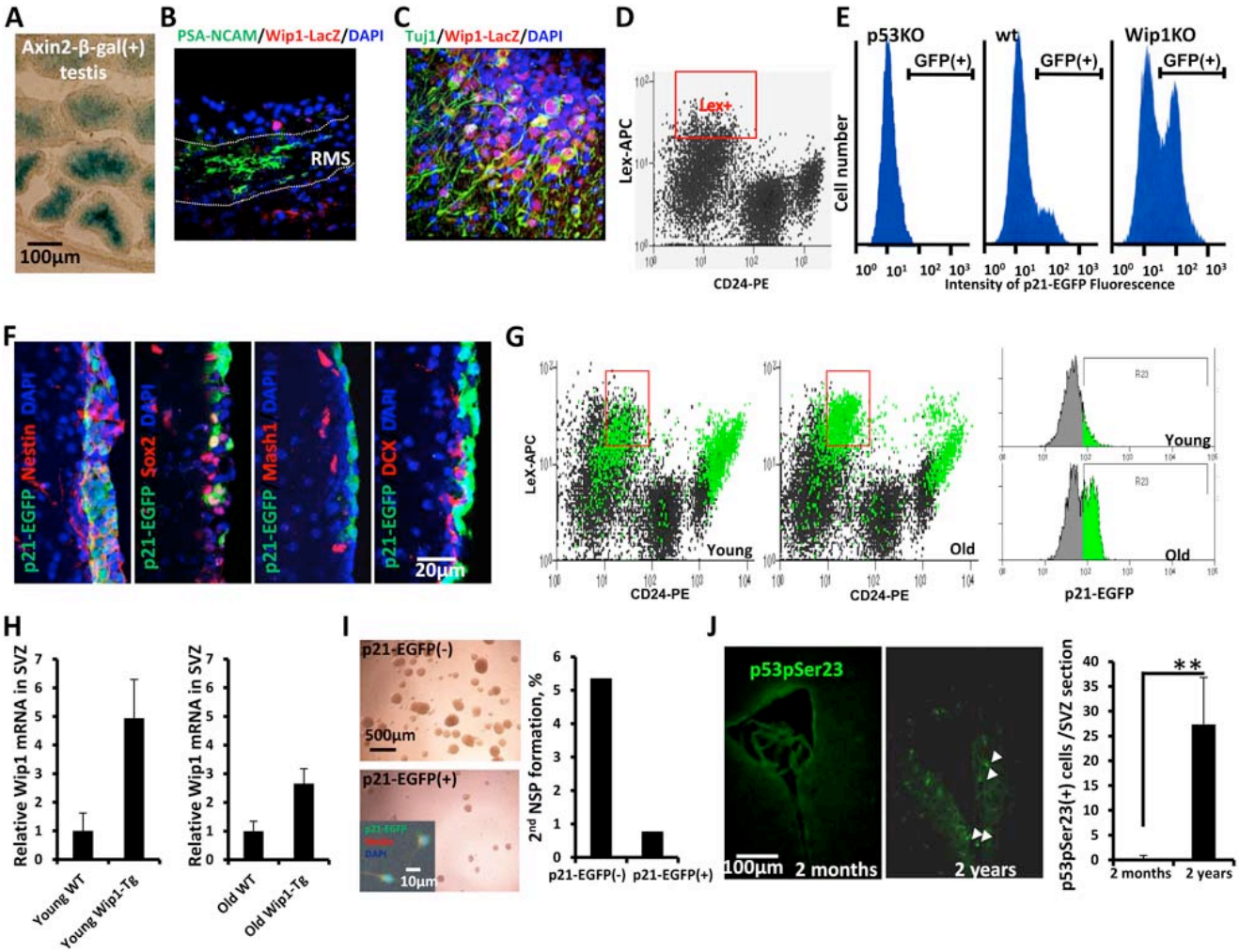

Figure S1. *Wip1* expression and p53 activity in NPCs.

(A) A representative photographs of β-galactosidase (β-gal) staining in testis.

(B) A representative image of *Wip1*-β-gal, which is absent in RMS.

(C) A representative image of *Wip1*-β-gal staining showing Wip1 is re-expressed on some cells at plexiform and Mitral cell layers.

(D) A representative image of isolating LeX -positive cells.

(E) FACS analysis of p21-EGFP-positive cells in primary NPCs derived from young *p53* KO, *wt* and *Wip1* KO mice.

(F) Representative images showing colocalization of p21-EGFP with NESTIN, SOX2, MASH1, and DCX. Note p21-EGFP signal is present only in NESTIN, SOX2- positive cells.

(G) Left, representative images of p21-EGFP signal over total population of 2 months and 1 years old LeX(+) cells. We found that p21-EGFP signal is present in ependymal cells (CD24 high) and some LeX -positive/CD24- negative cells. p21-EGFP signal increases from 4-

13% to 26-42% during aging as shown in the right and Figure **1E**.

(H) Left, *Wip1* mRNA expression is assessed in 2 months old *wt* and *Wip1*-Tg mice. Right, *Wip1* mRNA expression is assessed in 1 year old wt and *Wip1*-Tg mice. Data are mean±SEM.

(I) Left, Representative images of secondary NSPs formed from p21-EGFP negative (top panel) and positive (bottom panel) cells. Right, quantification of secondary NSP formation (right panel). An insert shows sorted p21-EGFP positive cells stained with NESTIN (red).

(J) Representative images of staining on phospho-Serine 23 of p53 (p53pSer23), an activated form of p53. Right, quantification of p53 pSer23-positive cells in the SVZ area. Data are mean±SEM. *, $p<0.05$; **, $p<0.01$; ***, $p<0.005$.

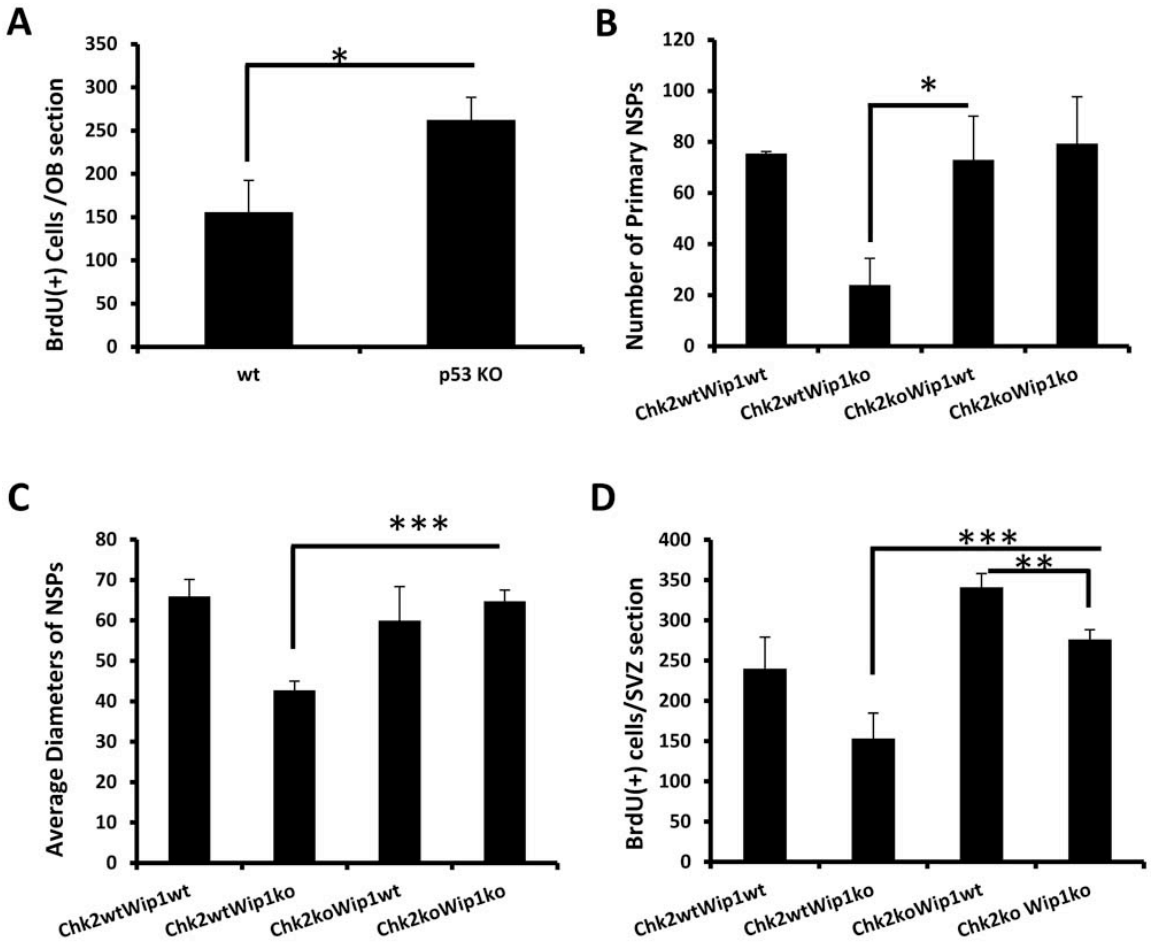

Figure S2. Characterization of neural stem cells in *Chk2* KO, *p53* KO and *Wip1*-Tg mice.

(A) Quantification of new cell formation in *wt* and *p53* KO olfactory bulb at 4-6 months of age. Data are mean±SEM.

(B) Quantification of the numbers of primary NSPs from *wt*, *Wip1* KO, *Chk2* KO and *Chk2* KO/*Wip1* KO mice. Note a reduced number of NSPs obtained from *Wip1* KO mice that is rescued by deficeincy of *Chk2*. Data are mean±SD.

(C) Quantification of the average diameter of primary NSPs from *wt, Wip1* KO, *Chk2* KO and *Chk2*/*Wip1* DKO mice. Note that the *Wip1* KO NSPs exhibit significantly reduced average size compare to wt mice. *Chk2* deficiency rescues this defect. Data are mean±SEM.

(D) Quantification of short-term BrdU incoporation in the SVZ of *wt, Wip1* KO, *Chk2* KO and *Chk2/Wip1* DKO mice. Note that the *Wip1* KO SVZ exhibits reduced short-term BrdU incorporation compared to that of wt mice that is rescued by *Chk2* KO. Data are mean±SEM. *, $p<0.05$; **, $p<0.01$; ***, $p<0.005$.

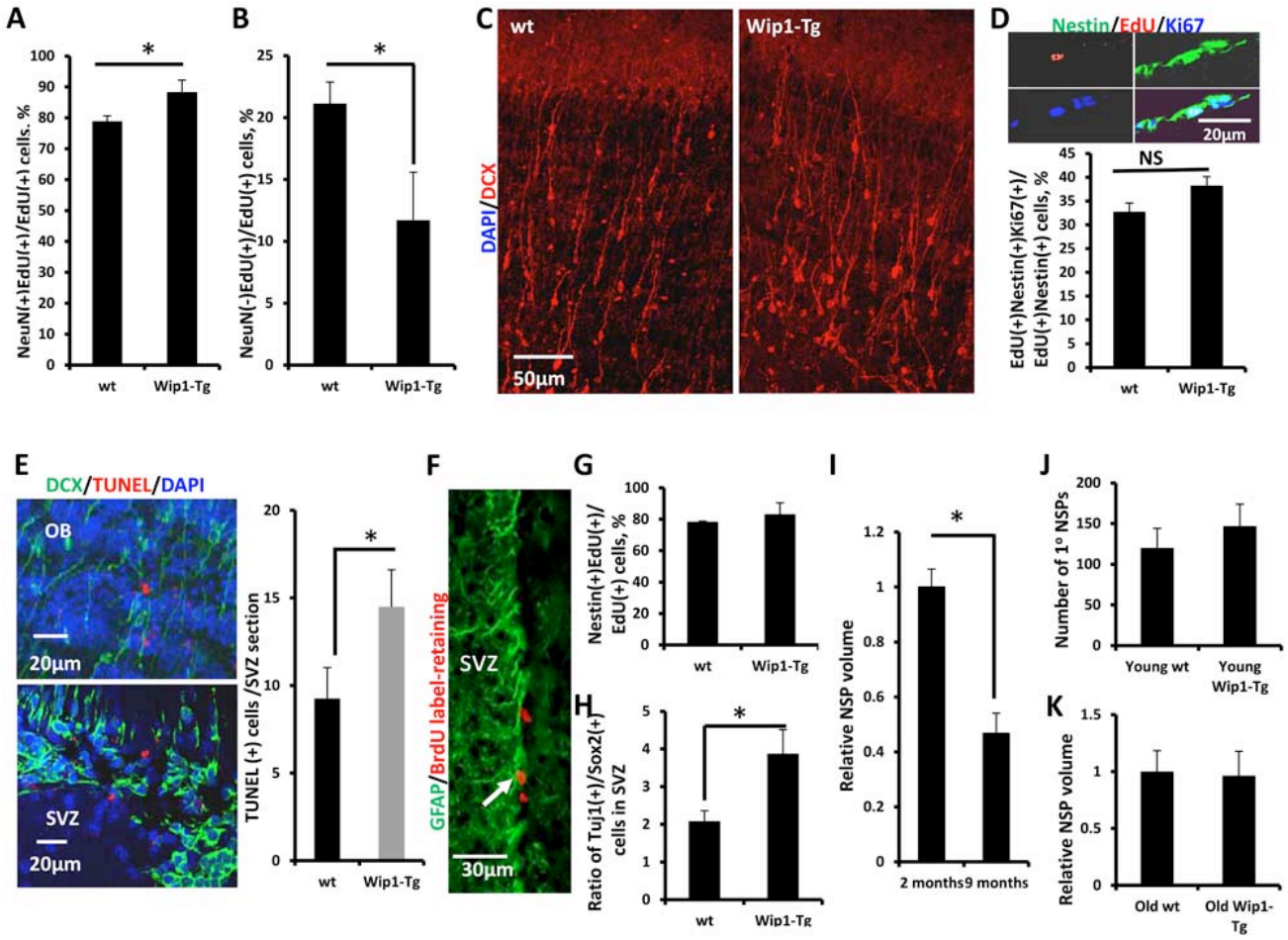

Figure S3. Additional analysis on new neuron formation in *Wip1*-Tg mice

(A) Quantification of NeuN-positive cells over total EdU-positive cells in aged (16-18 months) *wt* and *Wip1*-Tg mice. Data are mean±SEM.

(B) Quantification of NeuN-negative cells over total EdU-positive cells in aged (16-18 months) *wt* and *Wip1*-Tg mice. Data are mean±SEM.

(C) Representative images of DCX staining in OB of 18-month old *wt* and *Wip1*-Tg mice.

(D) Reprentative images (top) and quantifications (bottom) of a Nestin/EdU double positive cells that is positive for Ki67, 1 month after EdU injection. Data are mean±SEM.

(E) Left, TUNEL analysis double stained with DCX. Right, counting of total TUNEL positive cells in SVZ of 1 year old *wt* and *Wip1*-Tg mice. Data are mean±SEM.

(F) A representative image of LT-BrdU cells. The arrow highlights a BrdU-positive cell expressing GFAP, a stem cell marker in SVZ.

(G) Quantification of LT-EdU/Nestin double labeling shown in main Figure 2D. Data are mean±SEM.

(H) Ratio of Tuj(+) / Sox2(+) cells in 16-18 months old *wt* and *Wip1*-Tg SVZ. Data are mean±SEM.

(I) Quantification of the relative volume of NSPs of 2 and 9 months old mice. Data are mean±SEM.

(J) Quantification of the number of NSPs of 3-4 months *wt* and *Wip1*-Tg mice. Data are mean±SD.

(K) Quantification of the relative volume of NSPs of 16-18 months old *wt* and *Wip1*-Tg mice. Data are mean±SEM. *, $p<0.05$; **, $p<0.01$; ***, $p<0.005$.

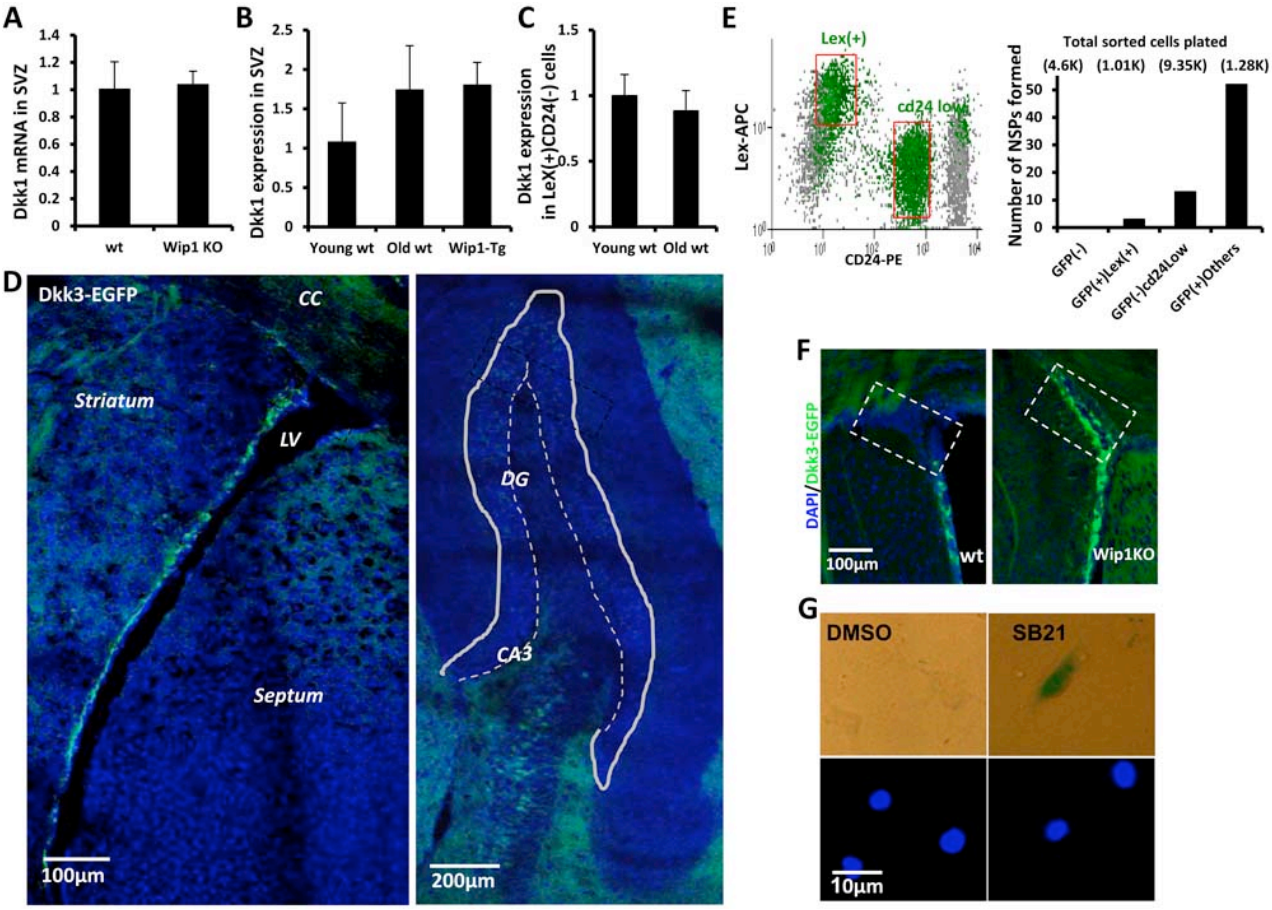

Figure S4. Analysis of *Dkk1* and *Dkk3* expression.

(A) Quantification of relative levels of *Dkk1* mRNA in SVZ. Data are mean±SD.

(B) Analysis on *Dkk1* mRNA in freshly isolated cells from SVZ region of young (3-4 months) and old (16-18 months) wt, and old (16-18 months) *Wip1*-Tg mice. Data are mean±SD.

(C) Analysis of *Dkk1* mRNA in FACS-sorted LeX(+)CD24(-) SVZ cells (right panel) from young (3 months) and middle age (8 months) wt mice. Data are mean±SD.

(D) A representative image of *Dkk3*-EGFP expression along the lateral ventricle (*LV*) and in hippocampus DG regions.

(E) Left, gating regime for sorting *Dkk3*-EGFP-positive and –negative cells from adult SVZ region. We collected cells from GFP(-), EGFP(+)LeX(+), EGFP(+)CD24(low), and the rest of EGFP positive cells for neurosphere assay. Right, quantification of neurospheres formation with with total number of initial sorted cells plated indicated on top of each bar. Note that LeX(-)CD24(-) cells are forming most of NSPs.

(F) Representative photographs of SVZ *Dkk3*-EGFP signal in young wt and W*ip1* KO

mice that carry *Dkk3*-EGFP transgene. Note that the increase of EGFP signal is evident throughout the SVZ region (red line boxed areas), but the increase is particularly evident in anteria SVZ (shown in dashed white line boxed areas).

(G) Representative images showing that upon SB21 treatment NPCs turn on *Axin2*-βgal signal. *, $p<0.05$; **, $p<0.01$; ***, $p<0.005$.